J Mater Sci (2011) 46:5790–5797
DOI 10.1007/s10853-011-5534-4

Influence of humidity on the scratch behavior of polystyrene–acrylonitrile random copolymers

Robert Browning · Rolf Minkwitz · Piyada Charoensirisomboon · Hung-Jue Sue

Received: 24 January 2011 / Accepted: 4 April 2011 / Published online: 12 April 2011

Abstract The effect of exposure to a humid environment on the scratch behavior of a set of model polystyrene–acrylonitrile (SAN) random copolymers was investigated over a period of 10 days. Linear increasing load scratch tests were performed according to ASTM D7027/ISO 19252. The critical loads for the onset of key scratch deformation mechanisms like periodic micro-cracking, plowing, and scratch visibility were used as metrics for evaluating scratch resistance. The scratching coefficient of friction was evaluated, as well. It was found that, in general, the scratch resistance decreases during the first few days of moisture exposure, but then experiences a degree of recovery upon saturation. It is proposed that the initially absorbed moisture causes plasticization, making the surface weaker until saturation where the water molecules gather together on the surface to impart a degree of lubrication and consequently improve the scratch resistance. Implications of moisture absorption on the scratch behavior of polymers will be discussed.

Introduction

The scratch behavior of thermoplastic polymers is gaining more and more attention due to an apparent increase in importance in both functional and esthetic applications, including, but not limited to, cellular phones, high-density televisions and monitors, and interior/exterior automobile fascia. Thermoplastic polymers are attractive for their light weight, recyclability, low cost, and the relative ease with respect to metals and ceramics in which they can be fabricated into just about any imaginable shape. Yet, the scratch resistance of thermoplastics is still weaker than that of rivaling ceramics or metals in esthetic applications, so there is a constant desire to improve their performance. Although there are a number of scratch test methods and respective material scratch performance specifications described for thermoplastics, for effective comparison and ranking, it is important to take into account any environmental effects.

One of the most common factors that would affect the surface properties of a material is exposure to the environmental conditions like ultraviolet (UV) radiation, cyclical heating/cooling, or a humid atmosphere. Polymers like polycarbonate, polystyrene, and polyether–ether ketone (PEEK) experience environmental stress cracking as a result of photo-degradation when exposed to the UV radiation of the sun [1–3]. Since polymers experience densification and embrittlement upon thermal aging, the heating and cooling cycle of a typical day can significantly affect the properties of polymers. Jiang et al. found that when exposed to the extreme environmental heating/cooling cycle conditions that reflect the summer conditions of Houston, Texas, multi-layer polyolefin/epoxy-based coatings will eventually experience cathodic disbondment which deletes their protective purpose [4].

Some research has been done probing the effects of environmental conditions on the tribological performance of polymers [5–11]. Myshkin [8] found that increasing the temperature gives an increase in friction, which influences the adhesive component and affects the deformation during the sliding process. An increase in temperature was found

R. Browning · H.-J. Sue (✉)
Polymer Technology Center, Department of Mechanical Engineering, Texas A&M University, College Station, TX 77843-3123, USA
e-mail: hjsue@tamu.edu

R. Minkwitz · P. Charoensirisomboon
BASF SE, Ludwigshafen, Germany

to have a detrimental effect on the scratch resistance of coated automobile polymer systems [9]. The environmental effects on the wear behavior of disc brake systems were investigated where the outside surrounding temperature can be on the order of −60 °C in Polish winters while the internal material temperature can sometimes reach 700 °C due to tribological friction [10]. Research involving silicone skin coated with polyacrylic acid-*graft*-polyethylene glycol (PAA-*g*-PEG) in sliding contact with artificial grass was carried out by van der Heide et al. to simulate sliding of human skin against grass in sports [11]. They found that the lubrication provided by water can reduce the friction coefficient from greater than one to less than 0.01.

With regards to surface deformation resistance, one of the most apparent environmental factors to be considered is the humidity to which a polymer is exposed to after being fabricated, usually through injection-molding, blow-molding, or extrusion. Polar thermoplastic polymers are susceptible to moisture absorption and diffusion due to their affinity to moisture and nanoporous nature. The absorbed moisture behaves as a sort of plasticizer for the polymer chains to exert a greater degree of freedom for chain movement, thus weakening the polymer. To our best knowledge, no controlled efforts have been undertaken to directly link the effect of absorbed moisture and material parameters on the scratch performance of polymers.

Plasticization is known to have a detrimental effect on properties like glass transition temperature, modulus, tensile strength, etc. [12–14]. There has been a great deal of work focused on the moisture absorption of cross-linked epoxy-based polymer matrices [15–17]. Moisture absorption of many thermoplastic polymers like polyethylene, polypropylene, and polystyrene, on the other hand, is considered largely negligible due to their highly non-polar nature in contrast to other thermoplastics which contain stronger polar groups. For instance, the oxygen atoms present in the backbone of polycarbonate impart a degree of polarity which allows the material to absorb ~0.35 wt% of water at 25 °C [18]. The acrylonitrile (AN) phase of polystyrene–acrylonitrile (SAN) consists of a highly polar carbon–nitrogen triple bond (C≡N, dipole moment = 3.9 Debye), which has a high affinity for environmental moisture. The equilibrium bulk moisture absorption for SAN as reported in the literature is on the order of one percent by weight at 25 °C [19].

It was shown recently how the scratch behavior of SAN is influenced by changing the amount of AN in the copolymer [20]. It was also found that increasing the AN content of the copolymer results in an increase in tensile strength and also improves the resistance to micro-cracking, plowing, and scratch visibility. However, increasing the AN content is expected to increase the amount of water absorbed by the copolymer. In fact, other authors have shown that changing the AN content of SAN changes the surface energy as measured via contact angle [21]. The same authors also showed that the amount of AN contained on the surface is expected to be higher than in the bulk as estimated through surface energy calculations. Therefore, the amount of AN in the copolymer is expected to influence its moisture absorption on the sample surfaces, thereby its scratch behavior.

The current work investigates the influence of moisture exposure on the scratch behavior of a set of model SAN random copolymer systems with varying AN content using a standardized progressive load scratch testing and analysis methodology (ASTM D7027/ISO 19252) [22, 23]. The onsets of scratch deformation mechanisms like scratch visibility, periodic micro-cracking within the scratch path, and plowing (fracturing away or machining of material by the scratch tip), as well as the scratch coefficient of friction (SCOF) are identified as metrics for scratch resistance evaluation. It is hoped that the current study can shed light on how an environmental factor, such as moisture uptake resulting from exposure to a humid environment, can influence the scratch behavior of polymers.

Experimental

Model SAN systems

BASF SE (Ludwigshafen, Germany) provided the SAN systems for this study in the form of reactor-grade random copolymers polymerized by free-radical reactions containing 19, 27, and 35 wt% AN. Physical properties of the model systems are summarized in Table 1. All properties were evaluated by BASF SE except for the diffusion coefficient which was obtained at Texas A&M University. The molecular weight was obtained from light scattering measurements and polydispersity is defined as M_w/M_n, as usual. It was verified that molecular weight imparts negligible influence on the moisture absorption behavior. Thus, only the effect of AN content is the focus of this investigation.

The SAN resins were produced into two sets of injection-molded samples. Small, transparent coupons with dimensions of 25.4 mm × 25.4 mm × 3 mm and a weight of ~1.5 g to

Table 1 Physical properties of SAN model systems

	SAN 19	SAN 27	SAN 35
Acrylontrile content (wt%)	19	27	35
Molecular weight (kg/mol)	134	119	104
Polydispersity	4.1	4.3	3.7
Equlibrium moisture uptake (%)	0.38	0.57	0.69
Diffusion coefficient (10^{-8} cm^2/s)	8.5	5.4	3.9

study the moisture absorption behavior while larger plaques with dimensions of 150 mm × 75 mm × 6 mm were used for the scratch study. For the larger plaques, 0.325% of anthrachinone and 0.15% of pyrazolone yellow were incorporated into the resins to create a sufficiently dark-colored material for scratch visibility analysis purposes. The surface finish of all plaques was smooth (RMS Roughness ≈ 65 nm) with a 60° specular gloss of 95 as measured with a BYK Gardner® Micro-TRI glossmeter.

Upon receipt, the injection-molded plaques were annealed between two smooth glass plates at 110 °C for 2 h to minimize residual stresses resulting from the injection-molding process. It was verified through profilometry with a Keyence® VK9700 violet laser scanning confocal microscope (VLSCM) that the surface finish was not affected by the annealing process.

Hygroscopic conditioning

All of the SAN samples were first dried overnight in an oven for 24 h at 80 °C and a vacuum pressure of 30 mmHg. After drying, the small coupons were weighed using a high precision digital scale. The samples were then placed in a sealed container with a dish holding sodium chloride salt and deionized water slurry. This provided a controlled environment with a relative humidity of ~75% at 23 °C. Over a period of 10 days, the small coupons were periodically removed from the humid environment and weighed. The percentage weight change from the dry condition was used to monitor the moisture absorption behavior.

Following the analysis of the moisture absorption behavior with the small SAN coupons, the scratch plaques were subjected to exposure in the humidity chamber and periodically scratch tested over a 10-day period. The effect of moisture absorption on the scratch behavior was analyzed by obtaining the critical load for the onset of key deformation mechanisms for SAN as described in [20].

Contact angle measurement

SAN systems containing 19 and 35 wt% AN were chosen to observe changes in contact angle as a function of moisture exposure time. Throughout conditioning, the samples were periodically removed from the humidity chamber and then placed on a flat, level surface for contact angle measurements. Single droplets of deionized water were deposited on each surface using a 1 ml syringe fitted with a 27.5 gauge needle. Images were obtained using the super macro mode of a 10 megapixel Olympus SP-570UZ camera. Images were processed (inverted and sharpened) using ImageJ (http://rsbweb.nih.gov/dij). Using the angle measuring tool in ImageJ, contact angles were measured for both sides of each droplet with respect to the sample surface. A minimum of six droplets was used to obtain average values. For reference, contact angles were measured for the dry condition, as well.

Scratch tests

Scratch tests were carried out according to the conditions outlined in ASTM D7027/ISO 19252 by using a progressive load range of 1–90 N at a constant scratch speed of 100 mm/s for a length of 100 mm. The scratch tip was made of stainless steel in a spherical geometry with a diameter of 1 mm. For each grade of SAN, all scratch tests were performed on the same plaque with three tests conducted for each periodic test. All tests were performed so that the tip movement was the same as the melt flow direction.

After the final scratch tests were completed (i.e., after 10 days of moisture exposure), 48 h was allowed for sufficient viscoelastic recovery of scratch deformation to take place before analysis was carried out. The plaques were then scanned using an Epson® Perfection Photo 4870 PC scanner at a resolution of 300 dpi. This resolution corresponds to the minimum feature size (~90 μm) that can be resolved by the average human eye [24]. A Munsell® minicolorchecker was scanned simultaneously with the samples for color correction with the ASV® software. A contrast level of 2% was used as the physiological criterion to correspond with the minimum level of contrast the human eye can perceive [24]. Using the feature size and contrast criteria, the onset of scratch visibility can be obtained using ASV® (http://www.surfacemachines.com). Since the orientation of the scratch path with respect to the illumination source can affect visibility assessment, the samples were scanned with the scratch path oriented perpendicular and parallel to the direction of light source travel in the scanner.

The scratch testing apparatus used in this work employs load cells that record the applied normal load and tangential force and sensors that read the horizontal and vertical displacement of the scratch tip. The critical load for the onset of any scratch deformation mechanism is found by first noting the distance along the scratch path where the damage first appears and then extracting the applied normal load at that point from the data file. The onset points for micro-cracking and plowing were directly observed under a light microscope. The SCOF is defined as the ratio of the applied normal load to the tangential force at each point for the duration of the scratch process. The SCOF is unique in that it takes into account both the usual concept of static and kinetic friction as well as the frictional forces that arise from resistance induced by the accumulation of material in front of the scratch tip [25].

Microscopic observation

A Keyence® VK9700 VLSCM was used for high-resolution analysis of the surface roughness and scratch damage mechanisms. The microscope is equipped with a 408 nm wavelength violet laser and has an *x*–*y*-axis resolution of ~120 nm while the height resolution is ~1 nm. The VK Analyzer software provided with the microscope was used to obtain optical images as well as topographical profiles. The tilt-correction and noise-filtering capabilities available in the software were used to process the raw images. RMS surface roughness was also measured using the VK Analyzer software. Details of the roughness measurement procedure can be found elsewhere [24]. The window for roughness measurement was circular with a diameter of 270 μm to correspond with the physiological resolution criterion of the human eye and to take into account continuity of scratch damage features.

An Olympus® BX60 optical microscope was used in reflection mode when high-resolution damage analysis was not required.

Results and discussion

Moisture absorption and diffusion behavior

The normalized weight gain for the SAN model systems is shown as a function of days of exposure to the humid environment in Fig. 1 and as a function of AN content in Fig. 2. In both figures, it can be seen that increasing the AN content increases the amount of water absorbed by the material. The AN content effect is initially only minimal upon 1 day of exposure, but then becomes more pronounced over the course of 3 days, after which the weight gain levels off. The values for the equilibrium moisture uptake are given in Table 1. Careful analysis suggests that the majority of the weight gained for all the systems occurred mostly within the first day of moisture exposure.

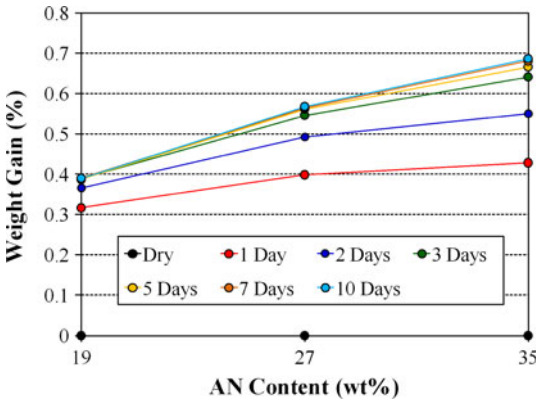

Fig. 2 Percentage weight change as a function of AN content for SAN systems

Initially, any moisture absorbed by the material is likely to be on the surface of the polymer. But as absorption continues, the moisture will diffuse into the polymer. The nature of the diffusion must first be understood before going further. To do so, the absorbed moisture at each time interval normalized against the saturation condition, $\frac{M_t}{M_{sat}}$, was calculated using the following equation:

$$\frac{M_t}{M_{sat}} = \frac{w_t - w_{dry}}{w_{sat} - w_{dry}} \quad (1)$$

where w_t, w_{sat}, and w_{dry} are the weight at time t, weight at saturation, and dry weight, respectively. The weight at saturation was calculated by averaging the weight values for several measurements after saturation had been observed. A plot of $\frac{M_t}{M_{sat}}$ versus the square root of exposure time, $t^{1/2}$, was constructed following the method of Shen and Springer [26] and is shown in Fig. 3. The data

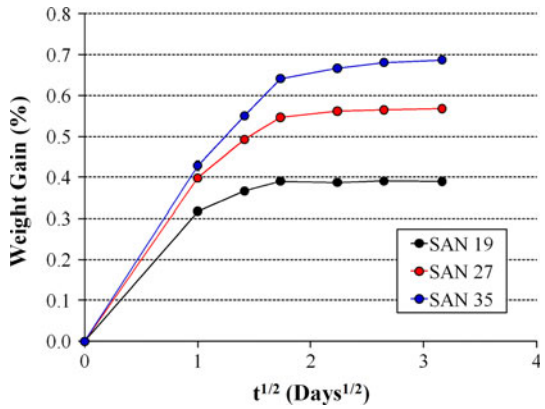

Fig. 1 Percentage weight gain as a function of time exposed to a humid environment for SAN model systems (R.H. = 75% at 23 °C)

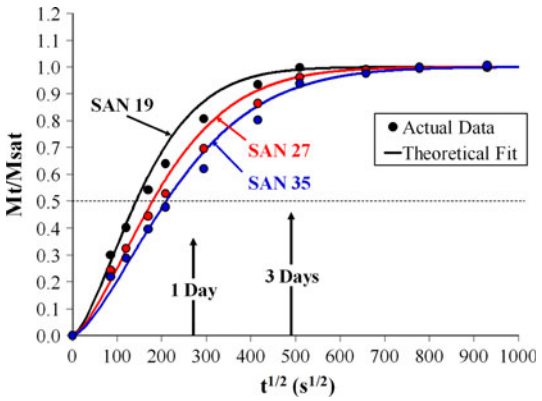

Fig. 3 Moisture absorption plot for SAN model systems

points have been fit to an approximate solution to Fick's second law as evaluated in [26]:

$$\frac{M_t}{M_{\text{sat}}} = 1 - \exp\left[-7.3\left(\frac{Dt}{l^2}\right)^{0.75}\right] \quad (2)$$

Figure 3 suggests that the diffusion is not likely completely Fickian in nature. Li et al. [16] stated that non-Fickian diffusion in bismaleimide resins can be attributed to hydrogen bonding between the water molecules and the matrix, as well as other factors. However, for comparison purposes, the diffusion coefficient, D, was approximated as in [27] by observing the time required to absorb half of the saturation limit:

$$D = \frac{0.049 \cdot l^2}{t_{1/2}} \quad (3)$$

The diffusion coefficients for each AN content level are given in Table 1. These values are close to the value of 3.4×10^{-8} cm^2/s reported by Bruder et al. [28] for SAN containing 28 wt% AN exposed to 50% R.H. at 23 °C. From these results, it can be concluded that increasing the AN content lowers the diffusivity. In other words, given a unit volume, if there are more AN groups within that unit volume, a longer time will be required to reach saturation, resulting from a lower diffusivity.

Contact angle measurement

As the surface of SAN absorbs moisture, the wettability of the surface is expected to change. Furthermore, a higher AN content is expected to reflect a higher affinity for moisture absorption, thus higher wettability. The contact angles for SAN 19 and 35 as measured with deionized water are shown in Fig. 4. As a basis of comparison, the values obtained in this study were compared to those obtained in the work done by Adão et al. [21]. The minor difference in magnitude of the two measurements is suspected to be due to the fact that the samples used by Adão et al. were films cast from methylene chloride whereas the current systems consist of injection-molded plaques.

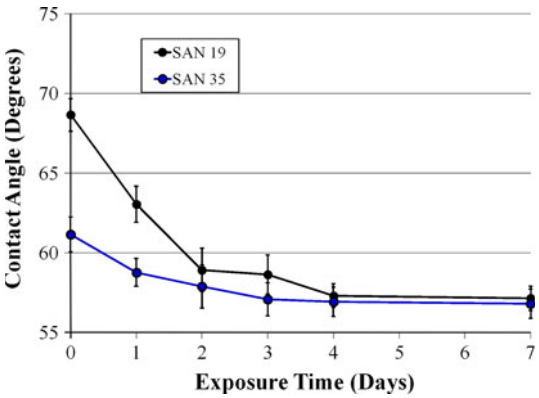

Fig. 4 Contact angle as measured with deionized water as a function of time exposed to a humid environment for SAN model systems

The expected behavior can be observed in the fact that a higher AN content does yield a lower contact angle, which implies higher surface polarity and greater wettability. With continued exposure, the contact angle decreases and then finally plateaus. Interestingly, the plateau values for both SAN 19 and 35 converge after equilibration of moisture absorption. This implies that the surface has indeed become saturated with water. The implications of this phenomenon will be elaborated upon later.

Scratch behavior

As stated before, the absorbed moisture is more than likely either on the surface or contained within a layer of the

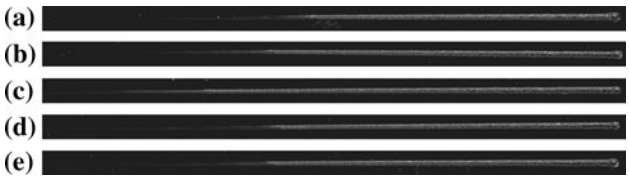

Fig. 5 Digitally scanned images of SAN 19 periodically scratch tested after being exposed to a humid environment, **a** dry, **b** 1 day, **c** 3 days, **d** 5 days, **e** 7 days (Resolution = 300 dpi, perpendicular orientation)

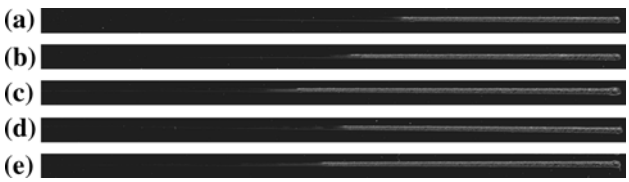

Fig. 6 Digitally scanned images of SAN 27 periodically scratch tested after being exposed to a humid environment, **a** dry, **b** 1 day, **c** 3 days, **d** 5 days, **e** 7 days (Resolution = 300 dpi, perpendicular orientation)

Fig. 7 Digitally scanned images of SAN 35 periodically scratch tested after being exposed to a humid environment, **a** dry, **b** 1 day, **c** 3 days, **d** 5 days, **e** 7 days (Resolution = 300 dpi, perpendicular orientation)

sub-surface, or both, and is expected to affect the scratch behavior of SAN significantly. Indeed, upon scratching, the scratch behavior of the exposed model SAN systems appears quite complex, as shown in Figs. 5, 6, and 7. It is readily evident from the visual results that there is a drastic change in the scratch behavior during the first 3 days of moisture exposure. That is, the scratch resistance appears to deteriorate with moisture absorption in the first 3 days and then begins to improve afterwards. This unusual behavior is most likely due to the fact that water molecules are first diffused into the sub-surface of the polymer, introducing a plasticizing effect which weakens the SAN and reduces its modulus and strength on the surface. Then, after saturation is reached, the water molecules form clusters on the surface which provides lubrication and slightly improves the scratch performance. Surface clustering of water molecules has been observed in the past for polycarbonate [18], polydimethylsiloxane and polymethylmethacrylate [29], epoxy matrices [30, 31] and even non-polymeric materials like Pd(111) [32].

Further evidence is shown by examining the critical load for the onset of the key deformation mechanisms for the SAN model systems: scratch visibility, periodic micro-cracking and plowing. Typical VLSCM micrographs showing the morphology of the micro-cracking and plowing features are shown in Fig. 8. Periodic micro-cracking in SAN is a result of the tensile stress that develops behind the scratch tip surpassing the ultimate tensile strength of the material [20]. The cracks are periodic in nature due to the well-known stick–slip phenomenon [33]. The authors define plowing as the point where the scratch tip has penetrated through the substrate and has begun to fracture or machine away the material in front of and around the tip. It has been observed that increasing the AN content generally imparts a significant degree of improvement to the overall scratch resistance of SAN random copolymers [20].

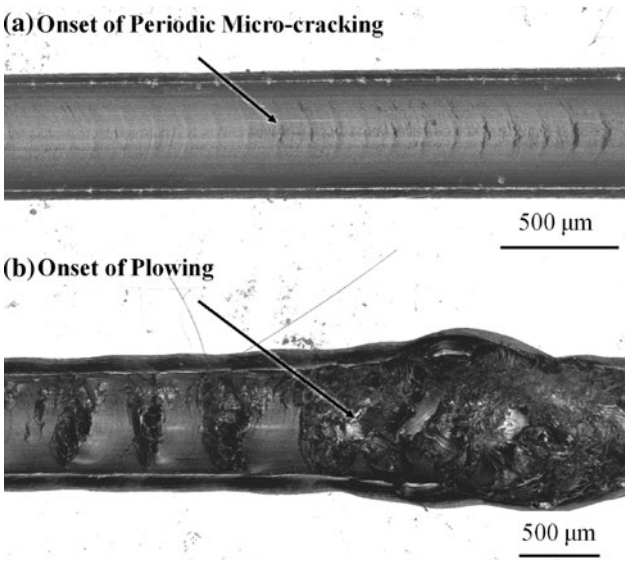

Fig. 8 Representative micrographs of SAN obtained via violet laser scanning confocal microscopy showing typical morphology of **a** periodic micro-cracking and **b** plowing

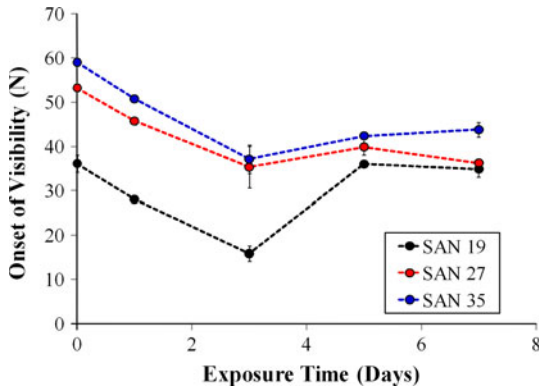

Fig. 9 Critical load for the onset of visibility in parallel illumination orientation for SAN model systems as a function of exposure time

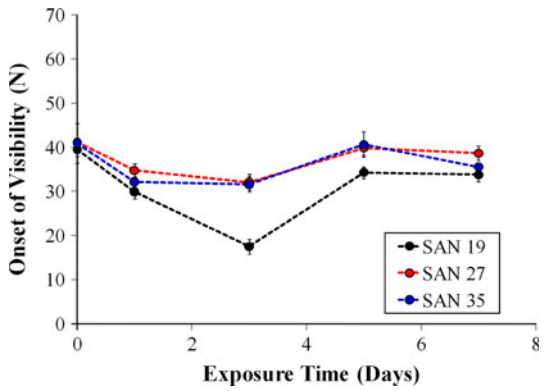

Fig. 10 Critical load for the onset of visibility in perpendicular illumination orientation for SAN model systems as a function of exposure time

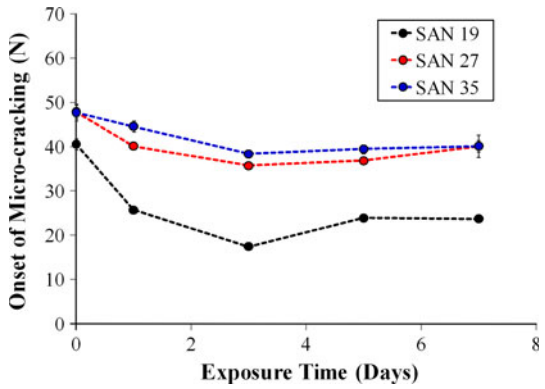

Fig. 11 Critical load for the onset of periodic micro-cracking for SAN model systems as a function of exposure time

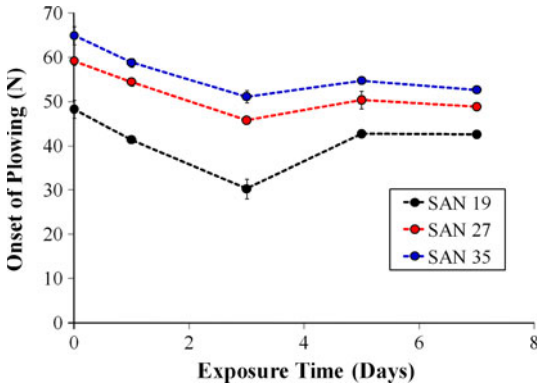

Fig. 12 Critical load for the onset of plowing for SAN model systems as a function of exposure time

The onset of the deformation mechanisms as a function of exposure time is given in Figs. 9, 10, 11, and 12. The mechanisms all appear to follow a similar trend; there is an initial degradation in the critical load up to the 3-day mark, followed by a slight recovery, especially for the SAN19 system. The exact reason why there is such a prominent effect observed in SAN19 is not currently known. It is proposed that due to its relatively low AN content, upon plasticization, the material behavior approaches that of polystyrene, which, from previous experience, has been observed to have poor scratch resistance compared to most polymers with respect to the damage mechanisms of this study. Then, after saturation is reached, the surface is lubricated by the absorbed moisture and the resistance improves rather substantially.

The SCOF is a measure of the ratio of the scratch-induced tangential force and applied normal load. The surface lubrication claim is supported by the curves in Fig. 13. The SCOF in the initial portion of the scratch displays a similar trend to the other key deformation mechanisms. It is highest at the 3-day mark and then becomes lower as exposure continues. It is known that a lower SCOF is associated with good scratch resistance [34, 35]. Therefore, since it is suspected that the absorbed moisture is at the surface after saturation, the supposed lubrication effect is highly likely.

It should be noted that the "spike" in the later portion of each of the SCOF curves corresponds to the onset of the plowing deformation mechanism. At this point, the tip penetrates the substrate and begins to machine away material from the scratch path. When this process first begins, there is a sudden increase in the tangential force due to the material pile-up in front of the tip. Once the machining process has begun, the tangential force lowers again. It can be observed from Fig. 13 that the location of these "spikes" follows the similar trend of degradation followed by recovery shown in Fig. 12.

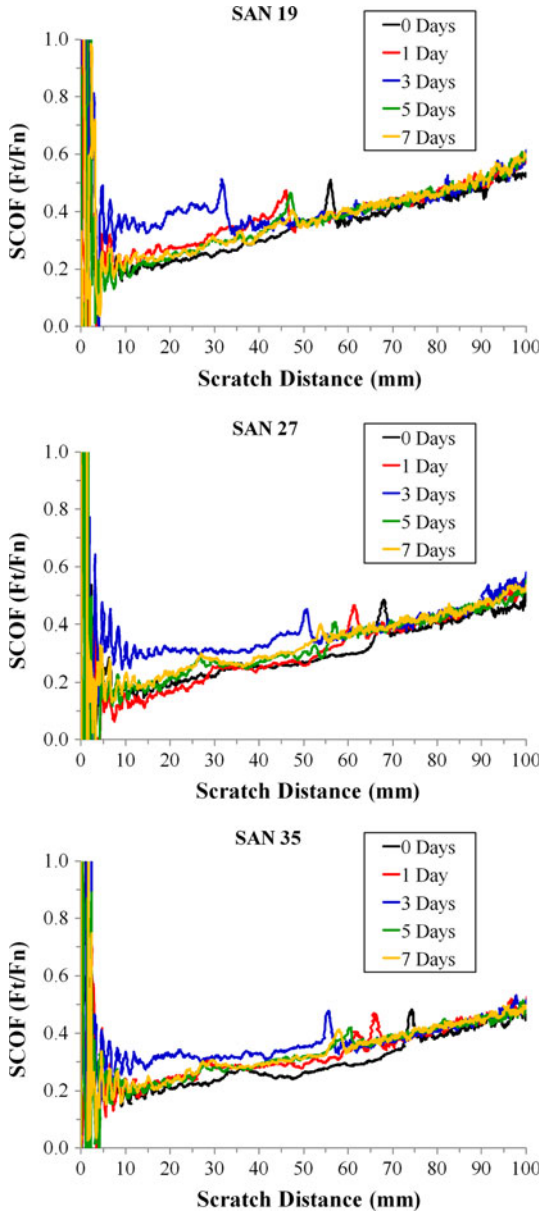

Fig. 13 Scratch coefficient of friction as a function of scratch distance for SAN model systems

The bulk mechanical properties of SAN are not expected to change much as a result of absorbed moisture. However, the surface properties would immediately be impacted, which would directly influence the scratch behavior. Obtaining experimental support for this claim is, unfortunately, rather difficult. More effort is underway to obtain direct evidence.

With regards to polymers in general, most thermoplastics do not present a great deal of concern with respect to changes in bulk behavior as a result of moisture absorption, even if there are polar functionalities present. However, the surface nature of the polymer can change greatly, which will in turn significantly influence the scratch behavior. The

more affinity the functional groups have for water molecules, the more the scratch behavior of the polymer is expected to change upon exposure to a humid atmosphere. Significant moisture absorption on the surface may strongly affect the deformation and damage mechanisms incurred for both brittle and ductile polymers in different fashions. Care should then be taken to make sure that exposure to a humid environment would not significantly compromise the scratch performance of the polymer of interest for any given application.

Conclusions

The scratch behavior of SAN random copolymer model systems with different levels of AN content was studied with regard to the influence of exposure to an environment maintained at 75% relative humidity and 23 °C over a 10-day period. Diffusion of environmental moisture into the SAN material occurs rapidly at first, reaching saturation after about 3 days. Equilibrium moisture uptake increased with AN content, the highest being $\sim$0.69 wt% for SAN with 35 wt% AN. A higher AN content also showed a lower contact angle under dry conditions, but after equilibration, the contact angle was the same, regardless of AN content. The scratch resistance was evaluated by monitoring the change in the onset of scratch deformation mechanisms like scratch visibility, periodic micro-cracking, and plowing using the methodology outlined in ASTM D7027/ISO 19252. During the initial stages of moisture exposure, scratch resistance decreased, which is attributed to plasticization of the material by the absorbed moisture. Upon moisture saturation on the surface, the scratch resistance experiences a degree of recovery, which is thought to be a result of water molecules clustering on the surface to serve as lubricant. This claim is corroborated by the SCOF measurement where the friction increases up to the saturation point, and then becomes lower thereafter. Care should therefore be taken for scratch research on polar polymers where surface moisture absorption is anticipated.

Acknowledgements The authors would like to thank both BASF SE and the Texas A&M Scratch Behavior of Polymers Consortium for the generous financial support of this work. Surface Machine Systems and the Polymer Technology Center are also given thanks for the use of their facilities and equipment. Thanks are given to Ehsan Moghbelli for the measurement of contact angles.

References

1. Timoteo GAV, Fechine GJM, Rabello MS (2008) Polym Eng Sci 48:2003
2. Sousa AR, Amorim KLE, Medeiros ES, Melo TJA, Rabello MS (2006) Polym Degrad Stab 91:1504
3. Nakamura H, Nakamura T, Noguchi T, Imagawa K (2006) Polym Degrad Stab 91:740
4. Jiang H, Browning R, Liu P, Chang TA, Sue H-J (2010) J Coat Technol 8:255
5. Rabek JF (1995) Polymer photodegradation: mechanisms and experimental methods. Chapman and Hall, London
6. Brostow W, Deborde J-L, Jaklewicz M, Olszynski P (2003) J Mater Ed 25:119
7. Brostow W, Kovacevic V, Vrsaljko D, Whitworth J (2010) J Mater Ed 32:273
8. Myshkin NK, Petrokovets MI, Kovalev AV (2005) Tribol Int 38:910
9. Hainsworth SV, Kilgallon PJ (2008) Prog Org Coat 62:21
10. Starczewski L, Szumniak J (1998) Surf Coat Technol 100:33
11. van der Heide E, Lossie CM, van Bommel KJC, Reinders SAF, Lenting HBM (2010) Tribol Trans 53:842
12. Cinquin J, Abjean P (1993) Int SAMPE Symp Exhib 1539
13. Biney PO, Zhong Y, Zhou J (1998) Int SAMPE Symp Exhib 43:120
14. Wilenski M (1997) PhD Thesis, Michigan State University
15. Li Y, Miranda J, Sue H-J (2001) Polymer 42:7791
16. Li Y, Miranda J, Sue H-J (2002) Polym Eng Sci 42:375
17. Lin YC, Chen X (2005) Polymer 46:11994
18. Bair HE, Johnson GE, Merriweather R (1978) J Appl Phys 49:4976
19. Smith WM (1958) Vinyl resins. Reinhold Publishing Corporation, New York
20. Browning R, Minkwitz R, Charoensirisomboon P, Sue H-J (2010) Polym Eng and Sci, DOI#22003
21. Adão MHVC, Saramago BJV, Fernandes AC (1999) J Colloid Interface Sci 217:94
22. ASTM D7027 (2005) ASTM International
23. ISO 19252 (2008) ISO International
24. Jiang H, Browning R, Fincher J, Gasbarro A, Jones S, Sue H-J (2008) Appl Surf Sci 254:4494
25. Jiang H, Whitcomb J, Sue H-J (2009) SPE TPO Conf, Sterling Heights, Michigan
26. Shen CH, Springer GS (1976) J Comp Mater 10:2
27. Hansen CM (1980) Polym Eng Sci 20:252
28. Bruder F, Haese W (1999) Jpn J Appl Phys 38:1709
29. Barrie JA, Platt B (1963) Polymer 4:303
30. Woo M, Piggott MR (1987) J Compos Technol Res 9:101
31. Karad SK, Jones FR (2005) Polymer 46:2732
32. Mitsui T, Rose MK, Fomin E, Ogletree DF, Salmeron M (2002) Phys Rev Lett 297:1850
33. Jiang H, Browning R, Sue H-J (2009) Polymer 50:4056
34. Browning R, Lim GT, Moyse A, Sun LY, Sue H-J (2006) Polym Eng Sci 46:601
35. Jiang H, Lim G-T, Reddy JN, Whitcomb JD, Sue H-J (2007) J Polym Sci B: Polym Phys 45:1435